THE JOURNAL OF PHYSICAL CHEMISTRY A

Article

pubs.acs.org/JPCA

Study on the Reaction of CH_2 with H_2 at High Temperature

Pei-Fang Lee, Hiroyuki Matsui,* and Niann-Shiah Wang*

Department of Applied Chemistry, National Chiao Tung University, 1001, Ta Hsueh Road, Hsinchu 30010, Taiwan

ABSTRACT: Thermal decomposition of CH_2I_2 [sequential C−I bond fission processes, $CH_2I_2 + Ar \rightarrow CH_2I + I + Ar$ (1a) and $CH_2I + Ar \rightarrow {}^3CH_2 + I + Ar$ (1b)], and the reactions of ${}^3CH_2 + H_2 \rightarrow CH_3 + H$ (2) and ${}^1CH_2 + H_2 \rightarrow CH_3 + H$ (3) have been studied by using atomic resonance absorption spectrometry (ARAS) of I and H atoms behind reflected shock waves. Highly diluted CH_2I_2 (0.1−0.4 ppm) with/without excess H_2 (300 ppm) in Ar has been used so that the effect of the secondary reactions can be minimized. From the quantitative measurement of I atoms in the 0.1 ppm CH_2I_2 + Ar mixture over 1550−2010 K, it is confirmed that two-step sequential C−I bond fission processes of CH_2I_2, (1a) and (1b), dominate over other product channels. The decomposition step (1b) is confirmed to be the rate determining process to produce ${}^3CH_2$ and the least-squares analysis of the measured rate gives, $\ln(k_{1b}/\mathrm{cm^3\ molecule^{-1}\ s^{-1}}) = -(17.28 \pm 0.79) - (30.17 \pm 1.40) \times 10^3/T$. By utilizing this result, we examine reactions 2 and 3 by monitoring evolution of H atoms in the 0.2−0.4 ppm CH_2I_2 + 300 ppm H_2 mixtures over 1850−2040 K. By using a theoretical result on k_2 (Lu, K. W.; Matsui, H.; Huang, C.-L.; Raghunath, P.; Wang, N.-S.; Lin, M. C. *J. Phys. Chem. A* **2010**, *114*, 5493), we determine the rate for (3) as $k_3/\mathrm{cm^3\ molecule^{-1}\ s^{-1}} = (1.27 \pm 0.36) \times 10^{-10}$. The upper limit of k_3 (k_{3max}) is also evaluated by assuming $k_2 = 0$, i.e., $k_{3max}/\mathrm{cm^3\ molecule^{-1}\ s^{-1}} = (2.26 \pm 0.59) \times 10^{-10}$. The present experimental results on k_3 and k_{3max} is found to agree very well with the previous frequency modulation spectroscopy study (Friedrichs, G.; Wagner, H. G. *Z. Phys. Chem.* **2001**, *215*, 1601); i.e., the importance of the contribution of ${}^1CH_2$ in the reaction of CH_2 with H_2 at elevated temperature range is reconfirmed.

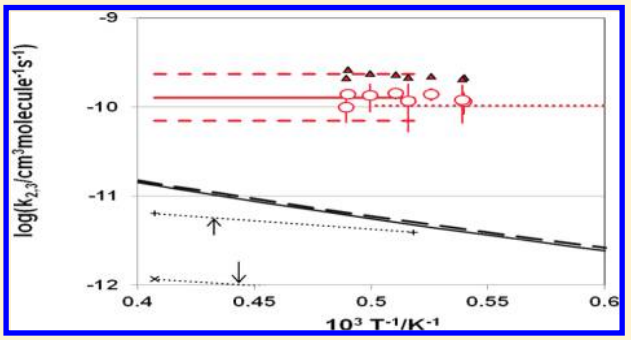

1. INTRODUCTION

The methylene radical, CH_2 ($\tilde{X}{}^3B_1$ and $\tilde{a}{}^1A_1$, represented as ${}^3CH_2$ and ${}^1CH_2$, respectively), is regarded as an important reaction intermediate in hydrocarbon combustion. In the standard combustion conditions, CH_2 radicals are supplied mostly in the secondary reactions such as $CH_3 + OH \rightarrow {}^1CH_2 + H_2O$ and sequential collisional quenching ${}^1CH_2 + M \rightarrow {}^3CH_2 + M$;[1−3] therefore, the higher the concentration of fuel species, the more important the role of CH_2. Also, it is indicated that ${}^1CH_2$ is a direct product in the thermal decomposition of CH_3OH.[2,3] In this case, CH_2 radical plays an important role in the initial stage of the chain branching processes even if the concentration of CH_3OH is low.

Detection of CH_2 radical has been tried by using various techniques (LMR spectrometers, mass spectrometers, infrared diode laser absorption for ${}^3CH_2$, and LIF and others for ${}^1CH_2$); a large amount of information about the rate constants and reaction mechanism of CH_2 radical have been accumulated at low temperature range.[4−21] Also, shock tube works combined with ARAS (atomic resonance absorption spectrometry) and the frequency modulation spectroscopy have been conducted to explore the CH_2 reactions above 1000 K.[22−25,36]

The main issue of this study is to obtain reliable kinetic information by monitoring evolution of H atoms produced in the reaction of $CH_2 + H_2$ at high temperature range. Highly sensitive detection of H atoms ($1 \times 10^{11}/\mathrm{cm^3}$) of this study would be efficient to reduce the effects of the side reactions. In addition, excellent reproducibility of the experimental condition in this shock tube system enables comparative measurement to confirm the concentration of the minor component in the sample mixture, as well as to examine the contributions of the background H atoms.

In most of the previous experimental studies, photolysis or thermal decomposition of CH_2CO has been used as a source of supplying CH_2. As CH_2CO is relatively stable below 2000 K, it is also the issue of the present study to search a clean source of producing CH_2 radical at lower temperature range. Therefore, this study is divided into two main experimental parts. In the first part, evolution of I atoms has been monitored by using VUV absorption at 178.3 nm in the mixture of 0.1 ppm CH_2I_2 + Ar over 1550−2010 K to examine the thermal decomposition process (1), i.e.,

$$CH_2I_2 + Ar \rightarrow CH_2I + I + Ar \quad (1a)$$

and

$$CH_2I + Ar \rightarrow {}^3CH_2 + I + Ar \quad (1b)$$

Received: October 5, 2011
Revised: January 16, 2012
Published: January 20, 2012

By using the result of thermal decomposition of CH_2I_2, we have examined the reactions

$$^3CH_2 + H_2 \rightarrow CH_3 + H \quad (2)$$

and

$$^1CH_2 + H_2 \rightarrow CH_3 + H \quad (3)$$

by monitoring H atoms. Even though $^3CH_2$ is expected to be the main products in (1b), it is important to take into account (3) at elevated temperature condition, as the collisional energy transfer between $^1CH_2$ and $^3CH_2$, (4) is very fast:

$$^1CH_2 + M = {}^3CH_2 + M \quad (4)$$

2. EXPERIMENTAL SYSTEM

Experimental study has been conducted behind reflected shock waves in a diaphragmless shock tube apparatus (length 5.9 m and i.d. 7.6 cm). Details of experiments were described in previous studies.[26,27] An atomic resonance absorption spectrometry (ARAS) detection system has been used for the measurements of temporal profiles of [I] and [H]; i.e., the resonant atomic absorption of I atoms at 178.3 nm (corresponding to transition $^2P_{1,3/2}-{}^2P_{0,3/2}$) and that of H atoms at 121.6 nm are monitored by a microwave-discharge lamp filtered with a vacuum UV (VUV) monochromator and detected by a solar-blind photomultiplier tube (PMT). A gas mixture of about 1% I_2 and H_2 diluted in He of 10 Torr is supplied in the microwave-discharge lamp. VUV light passes perpendicularly through the MgF_2 windows at 4 cm upstream of the end plate of the shock tube. In the measurement of I atoms, a solid iodine pellet cooled at 281 K is used to supply I_2. Calibration curves for H and I atoms have been constructed by using decomposition of C_2H_5I,

$$C_2H_5I + M \rightarrow C_2H_5 + I + M \qquad (\phi = 0.90 \pm 0.05)$$

and sequential decomposition of C_2H_5,

$$C_2H_5 \rightarrow C_2H_4 + H$$

Attention has been paid in the optical alignment to keep the sensitivity to be optimized; detection limit of 10^{11} atom/cm^3 for I and H atoms has been attained. In compensation for the achievement of high sensitivity, the resolution time of the detection is not sufficiently short for the measurements of very rapid reaction phenomena. By monitoring evolutions of I and H atoms in the thermal decomposition of C_2H_5I at 1900−2000 K and 2 atm, we measured the response time of the detection system to be about 25 μs.

However, the reliability of the observed evolutions of the signal intensities can be sufficiently retained (except for the initial 25 μs) if proper experimental conditions have been chosen; this is confirmed by analyzing evolutions of H atoms in the reaction of H + O_2 between 1700−2000 K in the mixtures of 0.2−0.4 ppm C_2H_5I + 300−500 ppm O_2.

The present experiment is conducted at very low concentration of sample mixtures, 0.1−0.4 ppm CH_2I_2 (and + 300 ppm H_2) diluted in Ar so as to reduce the influence of the side reactions; however, the sample mixtures are prepared simply by the measurement of pressure by using combination of Baratron pressure gauges.

He (99.9995%, AGA Specialty Gases), Ar (99.9995%, AGA Specialty Gases), and H_2 (99.9995%, AGA Specialty Gases) are used without further purification. CH_2I_2 (99%, Sigma-Aldrich, Reagent Plus grade) and C_2H_5I (99%, Sigma-Aldrich, Reagent Plus grade) are purified by repeating degassing by successive freezing and pumping cycles.

3. RESULTS AND DISCUSSIONS

3.1. Thermal Decomposition of CH_2I_2. Almost no kinetic information is available in the past literatures for CH_2I_2 decomposition. In the study on thermal decomposition of CH_2I_2, evolution of I atoms in the 0.1 ppm CH_2I_2 in Ar is monitored behind reflected shock waves over 1550−2010 K. Examples of the observed profile of [I] are demonstrated in Figure 1. As clearly shown, it is indicated that sequential two

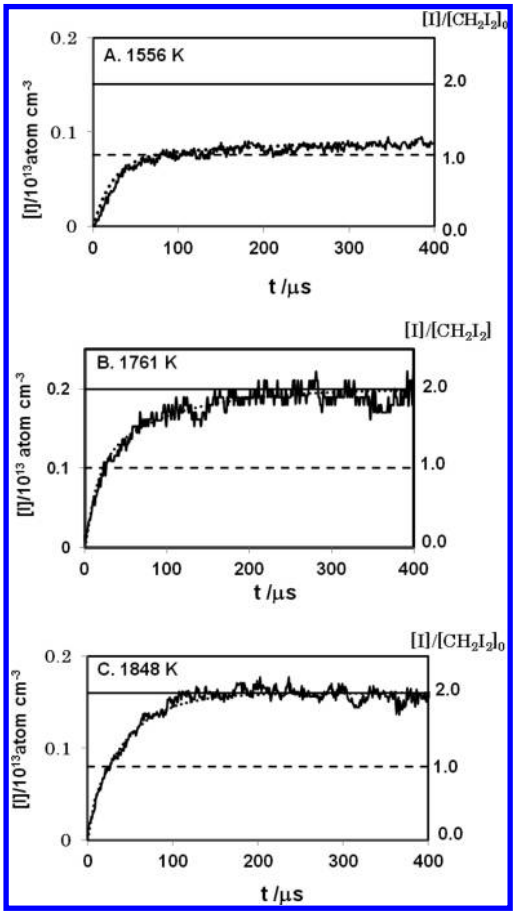

Figure 1. Examples of the observed evolution of I atoms in 0.1 ppm CH_2I_2 + Ar: (A) T = 1556 K, P = 2.16 atm, [Ar] = 1.02 × 10^{19}/cm^3; (B) T = 1761 K, P = 2.12 atm, [Ar] = 8.82 × 10^{18}/cm^3; (C) T = 1848 K, P = 2.08 atm, [Ar] = 8.26 × 10^{18}/cm^3. Calculated profiles of I atoms by using eq III is shown by the dotted curve, where the initial rise is given for (A) by using k_{1a} = 4.36 × 10^{-9} exp(−19858/T)/cm^3 molecule^{-1} s^{-1} (the rate for thermal decomposition of CH_3I, which has nearly equal dissociation energy with reaction 1a), and the rise rate given by the response time of the detection system was used for (B) and (C).

decomposition steps of C−I bond fission dominate over other product channels because it is shown at high temperature that $[I]_\infty/[CH_2I_2]_0 = 2$ (where $[I]_\infty$ and $[CH_2I_2]_0$ denote the concentrations of final iodine atoms and initial CH_2I_2, respectively). Also, the first decomposition step, $CH_2I_2 + Ar \rightarrow CH_2I + I + Ar$ (1a) is found to be very fast, in comparison with the second step, $CH_2I + Ar \rightarrow {}^3CH_2 + I + Ar$ (1b), exhibiting that the reaction intermediate CH_2I is stable even in the relatively high temperature range (T > 1500 K).

dx.doi.org/10.1021/jp211849h | J. Phys. Chem. A 2012, 116, 1891−1896

For the sequential decomposition of CH_2I_2, the profile of concentration of I atoms is analytically given by

$$[I]/[CH_2I_2]_0 = [1 - \exp(-R_1t)] + F_1[1 - \exp(-R_1t)] + F_2[1 - \exp(-R_2t)] \quad (I)$$

where $R_1 = k_{1a}(Ar)$, $R_2 = k_{1b}(Ar)$, $F_1 = R_2/(R_2 - R_1)$, and $F_2 = R_1/(R_1 - R_2)$. Because $R_1 \gg R_2$, the simple eq II is available in the analysis of the present experimental result,

$$[I]/[CH_2I_2]_0 = [1 - \exp(-R_1t)] + [1 - \exp(-R_2t)] \quad (II)$$

The observed initial rise rate of [I] is found to be too fast to evaluate k_{1a} in the temperature range above 1500 K. From the profile of I atoms in the range $1 < [I]/[CH_2I_2]_0 < 2$, the rate of (1b) was evaluated by using an estimated rate for R_1 into eq II[28] and the result is summarized in Table 1 as well as in Figure 2. Linear least-squares analysis of the data on k_{1b} gives

Table 1. Summary of the Experimental Condition for Thermal Decomposition of CH_2I_2 and the Rate Constant k_{1b}

T/K	P/atm	$[CH_2I_2]_0$[a]	[Ar][b]	k_{1b}[c]
1556	2.16	1.02	10.2	8.64×10^{-17}
1648	1.36	0.607	6.07	3.93×10^{-16}
1648	1.36	0.607	6.07	3.28×10^{-16}
1761	2.12	0.882	8.82	1.23×10^{-15}
1763	2.12	0.883	8.83	1.46×10^{-15}
1843	2.07	0.825	8.25	2.52×10^{-15}
1849	2.08	0.826	8.26	3.33×10^{-15}
1852	2.09	0.827	8.27	2.84×10^{-15}
1848	2.08	0.826	8.26	2.66×10^{-15}
2012	1.92	0.701	7.01	7.86×10^{-15}
2012	1.92	0.701	7.01	7.33×10^{-15}

[a]In 10^{12} molecule/cm^3. [b]In 10^{18} atom/cm^3. [c]In the unit of cm^3 molecule^{-1} s^{-1}.

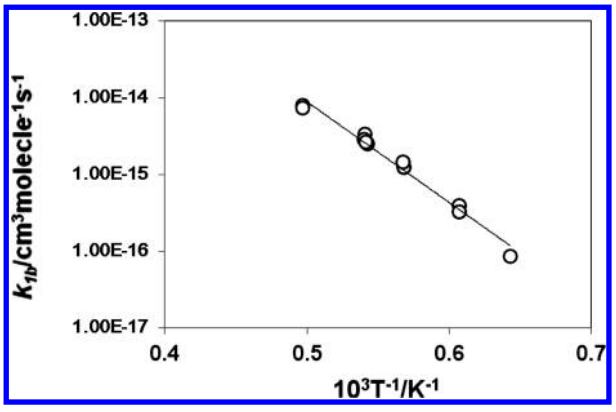

Figure 2. Arrhenius plot of the reaction rate for $CH_2I + Ar \rightarrow {}^3CH_2 + I + Ar$ (1b). Linear least-squares-analysis of the data is given by $k_{1b}/cm^3\ molecule^{-1}\ s^{-1} = 3.12 \times 10^{-8} \exp(-30170/T)$ and expressed by the straight solid line.

$$\ln(k_{1b}/cm^3\ molecule^{-1}\ s^{-1}) = -(17.28 \pm 0.79) - (30.17 \pm 1.40) \times 10^3/T \quad (III)$$

over the temperature range T = 1500−2000 K.

The heat of reaction is estimated as ΔH^0_{298} = 51.5 kcal mol^{-1} and ΔH^0_{298} = 64.4 kcal mol^{-1} for (1a) and (1b), respectively, on the basis of the recent experimental data on the heat of formation of CH_2I and the C − H bond fission energy.[29] The heat of reaction for other possible 3-centered reactions such as $CH_2I_2 + M \rightarrow CHI + HI + M$, $CH_2I_2 + M \rightarrow {}^{1,3}CH_2 + I_2 + M$, and $CH_2I + M \rightarrow CH + HI + M$, is estimated as ΔH^0_{298} = 72.5 kcal mol^{-1}, 79.1 kcal mol^{-1} (for the spin-forbidden $^3CH_2$ formation), and 93.9 kcal mol^{-1}, respectively.[30−33] Therefore, dominance of (1) over other channels, as well as two-steps production behavior of I atoms observed in this study can be justified thermodynamically. The observed activation energy of 60 kcal/mol for (1b) seems to be consistent with the endothermicity of the reaction.

CH_2I_2 is confirmed to be a clean and better source for supplying $^3CH_2$ than CH_2CO for the shock tube study below 2000 K; however, about 1800 K is indicated to be the lower limit for the purpose of quick supply. As (1b) is the rate determining step to produce $^3CH_2$, result III is used as the production rate for $^3CH_2$ in the analysis in the $CH_2 + H_2$ reaction in the following section. More detailed study on thermal decomposition of CH_2I_2 is now under way and will be presented elsewhere.[34]

3.2. Reaction of CH_2 with H_2. Evolution of [H] in the mixtures of 0.2−0.4 ppm CH_2I_2 + 300 ppm H_2 in Ar is monitored over 1850−2040 K. In conducting an experiment with very low concentration of sample gas such as employed in this study, it is especially important to examine the validity of the prepared concentration of minor component, as well as to confirm that the reaction system is free from the effect of impurities: these requirements may not be generally so easy to achieve when the concentration of sample gas is extremely low. As described above, the validity of the nominal concentration of CH_2I_2 prepared by pressure measurement has been confirmed here (because the measured yield of I atoms is equal to 2 times of the nominal concentration of CH_2I_2 for T > 1800 K). In addition, measurement of [H] in the CH_2I_2 + (excess H_2), as described below is useful to confirm this. These evidence ensure that the loss of CH_2I_2 should be negligible even for such low concentration samples.

The experimental condition of the present study is summarized in Table 2. All the data shown in the table are the averages

Table 2. Summary of the Experimental Conditions for CH_2 + H_2 Reaction and the Measured Rate Constants k_3 and k_{3max}

T/K	P/atm	[Ar][a]	$[CH_2I_2]_0$[b]	$10^{10}k_3$[c]	$10^{10}k_{3max}$[c]
0.4 ppm CH_2I_2 + 300 ppm H_2 + Ar					
2044	1.75	6.29	0.252	1.03 ± 0.33	2.14 ± 0.83
1958	1.99	7.45	0.298	1.44 ± 0.20	2.31 ± 0.73
1852	2.09	8.27	0.313	1.15 ± 0.31	2.16 ± 0.18
0.2 ppm CH_2I_2 + 300 ppm H_2 + Ar					
2041	1.86	6.69	0.134	1.40 ± 0.15	2.66 ± 0.47
2002	1.88	6.9	0.138	1.36 ± 0.47	2.39 ± 0.93
1938	2.01	7.62	0.152	1.17 ± 0.64	2.16 ± 0.30
1902	2.01	7.77	0.155	1.40 ± 0.19	2.21 ± 0.45
1855	2.08	8.23	0.165	1.21 ± 0.55	2.06 ± 0.83

[a]In 10^{18} atom cm^{-3}. [b]In 10^{13} molecule cm^{-3}. [c]In the unit of cm^3 molecule^{-1} s^{-1}.

of 2 data points conducted at the same shock wave condition; shot-by-shot fluctuation of the temperature shown in this table is less than ±5 K. Averaged values are shown for T and P. Repetition of the measurement at the same condition is useful to improve the S/N ratio (by signal averaging), as well as to confirm that reasonable reproducibility of the profiles of H atoms has been attained.

dx.doi.org/10.1021/jp211849h | J. Phys. Chem. A 2012, 116, 1891−1896

Also all the data shown in Table 2 are associated with blank tests using pure Ar and 300 ppm H_2 + Ar (both sample mixtures are prepared in the same condition with the mixture of 0.2−0.4 ppm CH_2I_2 + 300 ppm H_2 + Ar) to confirm that H atom is not supplied by impurities in Ar, H_2, nor the shock tube wall. Background H atom produced in the pure Ar sample was confirmed to be below the detection limit (1×10^{11} atom/cm^3) in all the experimental conditions, but a small amount of H atom production is observed (up to 5×10^{11} atom/cm^3) in the 300 ppm H_2 + Ar mixture at the highest temperature of this study: this is not from the impurities but it can be attributed to thermal decomposition of H_2.[1,35]

$$H_2 + Ar \rightarrow 2H + Ar \qquad (6)$$

An example of the observed profile of H atom produced in the mixtures of 0.2 ppm CH_2I_2 + 300 ppm H_2 is shown in Figure 3A.

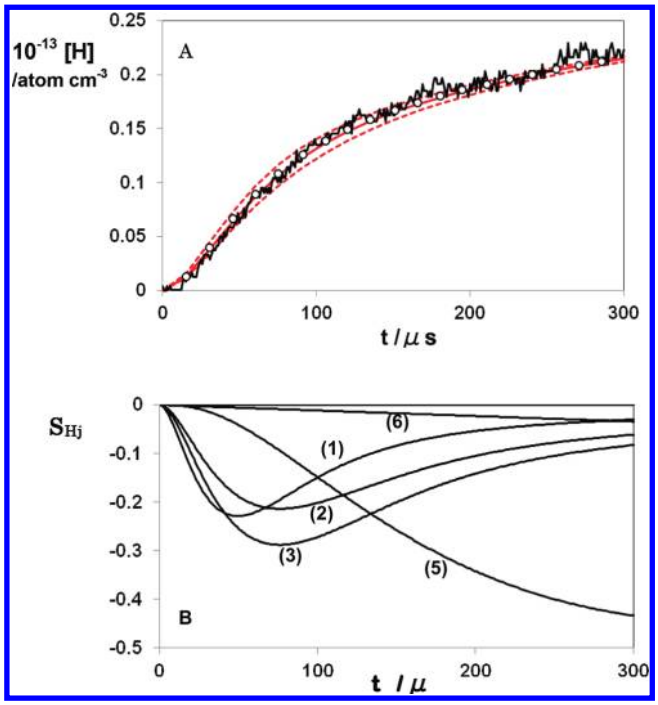

Figure 3. Example of the observed evolution of H atoms in the highly diluted CH_2I_2 + 300 ppm H_2 in Ar and comparisons with simulations. (A) Experimental result shown by the black solid line. Sample gas: 0.2 ppm CH_2I_2 + 300 ppm H_2 in Ar, T = 2002 K, P = 1.88 atm, [Ar] = 6.90×10^{18}/cm^3, $[CH_2I_2]_0 = 1.38 \times 10^{12}$/cm^3. Kinetic simulations using the mechanism of Table 2 are shown by the red solid curve and the values for ±30% of k_3 are shown by the red broken curves, respectively. The solution with the best fit of k_{3max} (maximum value for k_3 assuming $k_2 = 0$) is shown by the black open circle. (B) Sensitivity coefficient (nondimension) for H atoms; S_{Hj}, evaluated for the experimental condition of (A). The number indicated in this figure corresponds to the reaction number in the text and Table 3. The reactions in Table 3 not shown in this figure do not show any sensitivity.

Numerical simulations have been conducted to analyze the reaction rates of (2) and (3), however, it is practically impossible to evaluate k_2 and k_3 independently, because the collisional energy transfer from $^3CH_2$ to $^1CH_2$ (−4) is very fast and quasi-equilibrium between the two electronic states of CH_2 is maintained; two kinds of analyses have been tried in this study to estimate k_3 by assuming the magnitude of k_2, as described below.

The first approach of the analysis on k_3 here is to employ the result of theoretical calculation (ab initio molecular orbital and transition state theory, including Eckert correction) for the reaction (2) expressed as[27]

$$k_2/\text{cm}^3\ \text{molecule}^{-1}\ \text{s}^{-1} = 7.32 \times 10^{-19} T^{2.3} \exp(-3699/T)$$
$$T = 200-3000\ \text{K} \qquad (IV)$$

Using (IV) may be justified by the fact that (IV) agrees very well with the semiempirical data on k_2 based on the measurement of Gesser and Steacie[12] for the relative rate constant

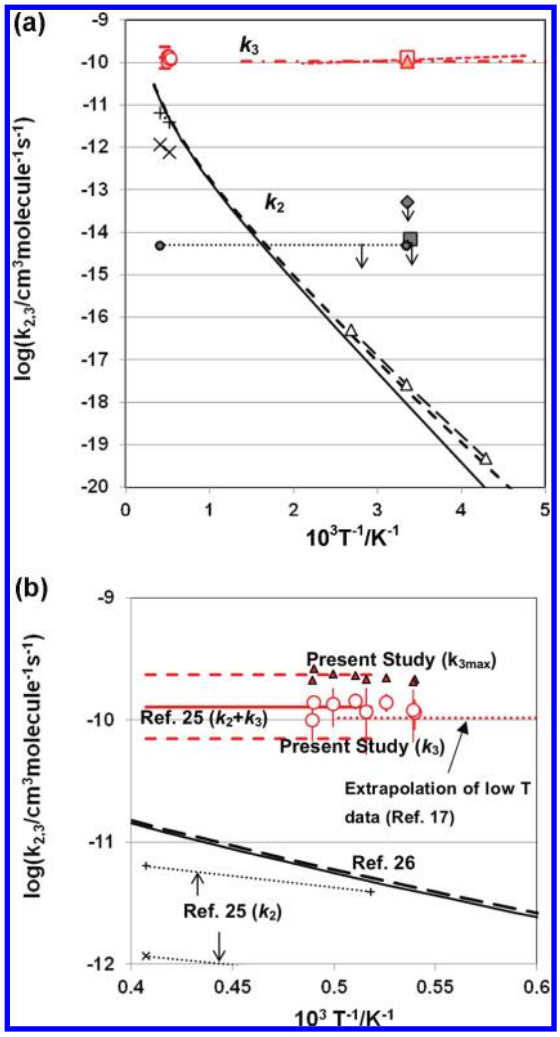

Figure 4. Summary of the reaction rates for $^3CH_2 + H_2 \rightarrow CH_3 + H$ (2) and $^1CH_2 + H_2 \rightarrow CH_3 + H$ (3). (A) k_2 (expressed by the black symbols): black solid line and black dashed line, TST calculation without Eckert correction and TST calculation with Eckert correction, respectively (ref 26); Δ connected by the black broken line, semiempirical result obtained by the relative measurement of k_2 combined with TST/quantum chemical calculation (refs 12 and 26); ■, ref 13; ◆, ref 14; dotted line, ref 16; × and +, ref 25. k_3 (expressed by the red symbols): red circle, present study; red solid line and red dashed line, ref 25 ($k_2 + k_3$); red dashed-dotted line, ref 17; red dashed line, ref 18; red square, ref 20; red triangle, ref 21. (B) k_2 (expressed by the black symbols): black solid line and black dashed line, TST calculation without Eckert correction and with Eckert correction, respectively (ref 21); × and + with dotted line, ref 25. k_3 (expressed by the red symbols): red circle, present study for k_3; red triangle, present study for the maximum value for k_3, i.e., k_{3max} (see text); red solid line, ref 25 ($k_2 + k_3$), where the upper and lower limits of ref 25 are shown by the red dashed lines; red dotted line, extrapolation of the low temperature study of ref 17.

dx.doi.org/10.1021/jp211849h | J. Phys. Chem. A 2012, 116, 1891−1896

Table 3. Reaction Mechanism for Analyzing the Observed Profile of the H Atom

reaction[a]	A^b	n^b	E^b	ref
1. $CH_2I_2 + M \rightarrow {}^3CH_2 + 2I + M$	3.12×10^{-8}	0	30170	this study
2. ${}^3CH_2 + H_2 = CH_3 + H$	7.32×10^{-19}	2.3	3699	26
3. ${}^1CH_2 + H_2 = CH_3 + H$	1.26×10^{-10}	0	0	this study
4. ${}^1CH_2 + M = {}^3CH_2 + M$	4.0×10^{-14}	0.9	0	15
5. $CH_3 + H_2 = CH_4 + H$	1.47×10^{-20}	2.74	4740	26
6. $2H + M = H_2 + M$ [c]	1.66×10^{-6}	−1	0	1
7. ${}^3CH_2 + CH_3 = H + C_2H_4$	1.89×10^{-10}	−0.1317	8.2	1
8. ${}^3CH_2 + CH_4 = 2CH_3$	4.09×10^{-18}	2	4164	1
9. ${}^1CH_2 + CH_3 = H + C_2H_4$	2.0×10^{-6}	0	−287	1
10. ${}^1CH_2 + CH_4 = 2CH_3$	2.66×10^{-11}	0	−287	1
11. $2CH_3 + M = C_2H_6 + M$ [d]	1.12×10^{-7}	−1.18	329.3	1
12. $CH_3 + CH_3 = C_2H_5 + H$	1.14×10^{-11}	0	5337	1
13. ${}^3CH_2 + {}^3CH_2 = C_2H_3 + H$	2.39×10^{-10}	0.0254	17.1	1
14. ${}^3CH_2 + {}^3CH_2 = C_2H_2 + H_2$	1.66×10^{-11}	0	0	1
15. $C_2H_5 + M \rightarrow C_2H_4 + H + M$ [d]	1.66×10^{-7}	0	15609	1
16. $C_2H_3 + M \rightarrow C_2H_2 + H + M$ [d]	4.98×10^{-9}	0	16113	1
17. ${}^3CH_2 + C_2H_6 = CH_3 + C_2H_5$	1.88×10^{-10}	0	3950	1
18. $CH_3 + C_2H_6 = CH_4 + C_2H_5$	1.02×10^{-17}	1.7	5262	1
19. $H + C_2H_6 = H_2 + C_2H_5$	1.91×10^{-16}	1.9	3792	1
20. $H + CH_3 + M = CH_4 + M$ [d]	2.31×10^{-9}	−0.534	270	1

[a]Forward and reverse reactions are considered when connected by "=". [b]$k = AT^n \exp(-E_a/RT)$ [molecule, cm^3, K, cal]. [c]Third-body collision efficiency for M (=Ar) is taken from ref 1. [d]Only parameters for the high pressure limit are shown but the rate for the falloff region is evaluated by using parameters given in ref 1.

for the reaction of ${}^3CH_2$ with H_2 (2) against

$$ {}^3CH_2 + CH_2CO \rightarrow {}^3C_2H_4 + CO \qquad \text{(reference reaction)} $$

combined with computed rate constant for ${}^3CH_2 + CH_2CO$[27] for the temperature range 230−370 K.

By using a reaction scheme shown in Table 3, we conducted fitting the numerical simulation to the observed profile for the evolution of H atoms in the range of initial fast rise for t = 25−150 μs, where the profile of H atoms is sensitive to the reactions ${}^3CH_2 + H_2 \rightarrow CH_3 + H$ (2) and ${}^1CH_2 + H_2 \rightarrow CH_3 + H$ (3). The optimized solutions for k_3, which give the best fit to the experimental profiles, are summarized in Table 2, and an example is shown by the red solid curve in Figure 3A.

The second approach of the present analysis is the limiting case evaluating the upper limit of k_3, i.e., k_{3max}, with an assumption $k_2 = 0$. As shown by the black circle in Figure 3A, it is possible to achieve good agreement of the numerical simulation to the experimental profile of H atoms even for neglecting the contribution of (2). The results of the analyses on k_{3max} are summarized also in Table 2.

An example of the computed sensitivity coefficients (nondimensional) are shown in Figure 3B. Contributions of the reactions in Table 3 other than (1)−(6) are in fact negligibly small, as the concentration of CH_2I_2 used in this study is very low. Contribution for the delay of producing ${}^3CH_2$ in the thermal decomposition of CH_2I_2 (1) is significant at the initial stage of the reaction, $CH_3 + H_2 \rightarrow CH_4 + H_2$ (5) dominates for large t, and the reaction (6) has some sensitivity at high temperature range, T > 2000 K, nevertheless, it is demonstrated that (2) and (3) are sufficiently sensitive to evaluate kinetic rate constant. It is also worthwhile to mention that the numerical simulation can reproduce very well the observed profile of H atoms with using the nominal value of the initial concentration of CH_2I_2 for all the experimental data; computation to estimate the accuracy for $[CH_2I_2]_0$ has been also performed and the nominal value is concluded to be reliable with ±10% error limit.

The present experimental result for (3) by employing theoretical result for k_2 can be expressed as

$$ k_3/\text{cm}^3\ \text{molecule}^{-1}\ \text{s}^{-1} = (1.27 \pm 0.36) \times 10^{-10} \qquad \text{(V)} $$

and the upper limit of k_3 (k_{3max}) by assuming $k_2 = 0$ can be expressed as

$$ k_{3max}/\text{cm}^3\ \text{molecule}^{-1}\ \text{s}^{-1} = (2.26 \pm 0.59) \times 10^{-10} \qquad \text{(VI)} $$

for the temperature range of T = 1850−2050 K, here, the error limit is given by 2σ.

The result of the present study on k_3 is compared with previous works on k_2 and k_3 in Figure 4A (summary of the data for a wide temperature range), and in Figure 4B (high temperature data including k_{3max}).

As shown in Figure 4A,B, the rate for (3) evaluated in this study is found to agree very well with that of previous shock tube work,[15] as well as with the experimental works below 1000 K.[17−20] Agreement of the high temperature data on k_3 with the experimental result by Gannon et al. conducted between 195−798 K[17] implies that k_3 shows almost no temperature dependence. Although the result by Friedrichs and Wagner[25] was indicated to be $k_2 + k_3$, it should be approximately equal to k_3, because the contribution of k_2 is indicated to be

dx.doi.org/10.1021/jp211849h | J. Phys. Chem. A 2012, 116, 1891−1896

minor. Their estimated upper limit for $k_2 + k_3$ also agrees very well with k_{3max} of this study.

As for reaction (2), it is difficult to examine k_2 precisely only from the present experimental information. The results on k_2 evaluated by Friedrichs and Wagner[25] are also shown in Figure 4, but it seems difficult to extract a reliable estimate because it should be very sensitive to the uncertainty of the magnitude of measured k_3.

The main conclusion of this study, in agreement with Friedrichs and Wagner,[25] is that the importance of $^1CH_2$ in the reaction of $CH_2 + H_2$ has been confirmed; i.e., the reaction at elevated temperature can proceed through collisional excitation from $^3CH_2$ to $^1CH_2$ if the reaction rate of $^3CH_2$ is not extremely large. The same scenario may hold for the reactions of CH_2 with other molecules. Gannon et al.[17] demonstrated in the study of $^1CH_2 + D_2$ reaction that an insertion reaction can be competitive to the direct abstraction reaction, because they confirmed that two-thirds of the products of this reaction was H atom. For the molecules other than H_2, insertion reaction can still be a part of the main channels for the thermal reactions of CH_2 at elevated temperature. Examination of the relative contributions of $^3CH_2$ and $^1CH_2$ in many of the key reactions in combustion system seems to be still a challenging task.

AUTHOR INFORMATION

Corresponding Author

*E-mail: N.S.W., nswang@nctu.edu.tw; H.M., matsui@tut.ac.jp.

Notes

The authors declare no competing financial interest.

ACKNOWLEDGMENTS

This work was supported by National Science Council of Taiwan under grant no. NSC 99-2113-M-009-014. H.M. deeply acknowledges the supports by NSC and National Chiao Tung University for a distinguished visiting professorship.

REFERENCES

(1) Smith, G. P.; Golden, D. M.; Frenklach, M.; Moriarty, N. W.; Eiteneer, B.; Goldenberg, M.; Bowman, C. T.; Hanson, R. K.; Song, S.; Gardiner; et al. http://www.me.berkeley.edu/gri mech.

(2) Xia, W. S.; Zhu, R. S.; Lin, M. C.; Mebel, A. M. *Faraday Discuss.* **2002**, *119*, 191−205.

(3) Srinivasan, N. K.; Su, M.-C.; Michael, J. V. *J. Phys. Chem. A* **2007**, *111*, 3951−3958.

(4) Böhland, T.; Temps, F.; Wagner, H. G. *Ber. Bunsen-Ges. Phys. Chem.* **1984**, *88*, 455−458.

(5) Seidler, V.; Temps, F.; Wagner, H. G.; Wolf, M. *J. Phys. Chem.* **1989**, *93*, 1070−1073.

(6) Böhland, T.; Temps, F.; Wagner, H. G. *Proceedings of the 2Ist Symposium (International) on Combustion*; The Combustion Institute: Washington, DC, 1988; pp 841−850.

(7) Kraus, H.; Oehlers, C.; Temps, F.; Wagner, H. G.; Wolf, M. *Ber. Bunsen-Ges. Phys. Chem.* **1989**, *97*, 545−553.

(8) Böhland, T.; Heberger, K.; Temps, F.; Wagner, H. G. *Ber. Bunsen-Ges. Phys. Chem.* **1989**, *93*, 80−87.

(9) Heberger, K.; Temps, F.; Volker, S.; Wolf, M.; Wagner, H. G. *Proceedings of the 23rd Symposium (International) on Combustion*; The Combustion Institute: Washington, DC, 1991; pp 29−35.

(10) Goldbach, A; Temps, F.; Wagner, H. G. *Ber. Bunsen-Ges. Phys. Chem.* **1990**, *94*, 104−110.

(11) Darwin, D. C.; Young, A. T.; Johnston, H. S.; Moore, C. B. *J. Phys. Chem.* **1989**, *93*, 1074−1078.

(12) Gesser, H.; Steacie, E. W. R. *Can. J. Chem.* **1956**, *34*, 113−122.

(13) Darwin, D. C.; Moore, C. B. *J. Phys. Chem.* **1995**, *99*, 13467−13470.

(14) Pilling, M. J.; Robertson, J. A. *J. Chem. Soc., Faraday Trans. 1* **1977**, *73*, 968−984.

(15) Brown, W.; Bass, A. M.; Pilling, M. *J. Chem. Phys.* **1970**, *52*, 5131−5143.

(16) Tsang, W.; Hampson, R. F. Chemical kinetic data base for combustion chemistry. Part I. Methane and related compounds. *J. Phys. Chem. Ref. Data* **1986**, *15*, 1087−1279.

(17) Gannon, K. L.; Blitz, M. A.; Pilling, M. J.; Seakins, P. W.; Klippenstein, S. J.; Harding, L. B. *J. Phys. Chem. A* **2008**, *112*, 9575−9583.

(18) Böhland, T.; Temps, F.; Wagner, H. G. *J. Phys. Chem.* **1987**, *91*, 1205−1209.

(19) Sosa, C.; Schlegel, H. B. *J. Am. Chem. Soc.* **1984**, *106*, 5847−5852.

(20) Ashfold, M. N. R.; Fullstone, M. A.; Hancock, G.; Ketley, G. W. *Chem. Phys.* **1981**, *55*, 245−257.

(21) Langford, A. O.; Petek, H.; Moore, C. B. *J. Chem. Phys.* **1983**, *78*, 6650−6659.

(22) Dombrowsky, Ch.; Wagner, H. G. *Ber. Bunsen-Ges. Phys. Chem.* **1992**, *96*, 1048−1056.

(23) Dombrowsky, Ch.; Hwang, S. M.; Rohrig, M.; Wagner, H. G. *Ber. Bunsen-Ges. Phys. Chem.* **1992**, *96*, 194−198.

(24) Frank, P.; Bhaskaran, K. A.; Just, Th. *J. Phys. Chem.* **1986**, *90*, 2226−2231.

(25) Friedrichs, G.; Wagner, H. G. *Z. Phys. Chem.* **2001**, *215*, 1601−1623.

(26) Lu, K. W.; Matsui, H.; Huang, C.-L.; Raghunath, P.; Wang, N.-S.; Lin, M. C. *J. Phys. Chem. A* **2010**, *114*, 5493−5502.

(27) Wu, C.-W.; Matsui, H.; Wang, N.-S.; Lin, M. C. *J. Phys. Chem. A* **2011**, *115*, 8086−8092.

(28) Kumaran, S. S.; Su, M.-C.; Michael, J. V. *Int. J. Chem. Kinet.* **1997**, *29*, 535−543.

(29) Seetula, J. A. *Phys. Chem. Chem. Phys.* **2002**, *4*, 455−460.

(30) Lias, S. G.; Bartmess, J. E.; Liebman, J. F.; Holmes, J. L.; Levin, R. D.; Mallard, W. G. *J. Phys. Chem. Ref. Data* **1988**, *17* (Suppl. 1), 1−861.

(31) Kudchadker, S. A.; Kudchadker, A. P. *J. Phys. Chem. Ref. Data* **1976**, *5*, 529−530.

(32) Furuyama, S.; Golden, D. M.; Benson, S. W. *J. Phys. Chem.* **1968**, *72*, 4713−4715.

(33) Carson, A. S.; Laye, P. G.; Pedley, J. B.; Welsby, A. M. *J. Chem. Thermodyn.* **1993**, *25*, 261−269.

(34) Lee, P.-F.; Matsui, H.; Chen, W.-Y.; Wang, N.-S. Manuscript under preparation.

(35) Warnatz, J. In *Combustion Chemistry*; Gardiner, W. C., Ed.; Springer-Verlag: Berlin, 1984; Chapter 5.

(36) Deppe, J.; Wagner, H. G. *Z. Phys. Chem.* **2001**, 1501−1526.